

Aerodynamic-Shape Optimization of Supersonic-Missiles Using Monte-Carlo

Ahmed Z. Al-Garni¹, Ayman H. Kassem², Ayman M. Abdallah³

Abstract –This paper presents a fast and reliable technique for aerodynamic shape optimization of supersonic missiles using Monte Carlo optimization method. The technique is based on two modules: Aerodynamics module and optimization module. The aerodynamic module is based on components build-up method where analytical, and semi-empirical of different missile components were added together, with some interference factors, to calculate the overall aerodynamics of the missile. The Aerodynamics module is validated against known wind tunnel data and showed good agreement. The optimization module is aimed at finding Missile geometry (such as length, fins dimensions and fins location, etc.) which maximize lift-over-drag using Monte Carlo technique. Monte Carlo simulation Technique has proved itself as a simple and easy to implement tool for aerospace vehicles shape optimization.

Keywords: Analytical aerodynamic model, component build-up method, Monte Carlo, missile shape configuration optimization, supersonic

I. Introduction

The missile aerodynamic geometry has high impact on different missile systems such as control, propulsion, structure, and warhead. Missile aerodynamicists aim to find the optimal external aerodynamic configuration. Missiles have to travel at varying speeds. The optimal aerodynamic configuration has to work efficiently at these variable speeds. The optimization process requires many iterations which makes computationally-expensive CFD models unappealing to be used in such calculations. A fast and reliable method such as build-up components method is used to predict performance for supersonic missiles quickly and reliably [1] [2] and [3].

Keshavarz [4] presented formulations for different multidisciplinary design optimization (MDO) and two MDO formulations are applied to a sounding missile in order to optimize the performance. Three disciplines have been considered, trajectory, propulsion and aerodynamics.

Sooy and Schmidt [5] presented a study on aerodynamic predictions, comparisons and validations using Missile Datcom (97) and Aeroprediction 98 (AP98) numerical prediction codes. They evaluated the accuracy of each code compared to experimental wind-tunnel data for a variety of missile configurations and flight conditions. The missile configurations included axisymmetric body, body wing tail and body tail. The results of this paper were used to validate the aerodynamic model used in this study.

The objective of the current paper is to present a fast and reliable technique for obtaining supersonic missile aerodynamics and use this technique for finding optimal

supersonic missile shape based on best performance (i.e. maximum lift-over-drag). Monte Carlo optimization [6] and [7] has been used in this work for its many attractive features such as robustness, global optimization, and simplicity of implementation.

II. Aerodynamic Model

The overall missile aerodynamic loads are calculated by summing up the aerodynamic characteristics of the major components separately (e.g., body, wing, tail, etc...) and then adding components interference factors. The missile's configuration here is composed of an axisymmetric forebody, a cylindrical after body, and two sets of in-line cruciform fins. This method is valid for Mach number range ($1.5 < M \leq 6$).

II.1. Normal Force Prediction

Missile's body can be divided into three main parts: the forebody (or nose), the mid-section, and the aft (or boattail). There are many forebody shapes, but the conical, ogival and power series (or hemispherical) shapes are the most commonly used. They are selected on the basis of combined aerodynamic, guidance, and structural considerations.

From the cross flow theory formulated by Allen and Perkins from [8], an accurate prediction of the normal force coefficient of the body is:

$$C_{Nb} = 2\alpha + \frac{4C_{\lambda_{cyl}}}{\pi} \alpha^2 \quad (1)$$

Where: α is the angle of attack, λ_{cyl} is defined as the cylinder fineness ratio ($\lambda_{cyl} = L_{cyl} / d$, missile's cylinder length over missile's diameter, Fig. 1) and C is a constant depends on the flow type, i.e.

$$C = \begin{cases} 1.2 & \text{For Laminar Flow} \\ 0.3-0.4 & \text{For Turbulent Flow} \end{cases}$$

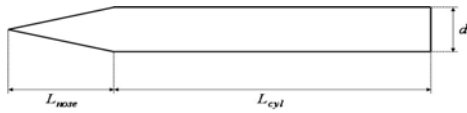


Fig. 1. Definition of missile body shape

Missile surface platforms include wing, tail, and canard surfaces. These may be fixed or movable (i.e., control surfaces). The surface normal force coefficient is a function of Mach number, local angle of attack, aspect ratio, and the surface platform area. C_N , which is based on the missile reference area, decreases with increasing supersonic Mach number and increases with angle of attack and the wing surface area. The normal force coefficient derivative for rectangular platform wing finite span with no sweep is [8]:

$$C_{N\alpha} = -\frac{4}{\sqrt{M^2 - 1}} \times \left[1 - \frac{1}{2AR\sqrt{M^2 - 1}} \left(1 - \frac{\gamma M^4 + (M^2 - 2)^2}{2(M^3 - 2)^{3/2}} A^1 \right) \right] \quad (2)$$

Where: M is the Mach number, AR is the aspect ratio for the wing or tail and A^1 is related to thickness to chord ratio (t/c) and is given in Table 1.

TABLE 1
DEFINITION OF A^1

Airfoil Type	Airfoil Shape	A^1
Double Wedge		$1/2(t/c)$
Modified Double Wedge		$2/3(t/c)$
Biconvex		$2/3(t/c)$

From [1] [9] and [14] the missile's total normal force coefficient after adding up all the components is:

$$C_N = C_{Nb} + C_{Nwa} (K_w + K_b)_w K_1 \alpha A_w + C_{Nwa} \left[(K_w + K_b)_t \alpha + (k_w + k_b)_m \sigma \right] K_2 \left(1 - \frac{d\varepsilon}{d\alpha} \right) A_t \quad (3)$$

Where: σ is the tail deflection angle. $(K_w + K_b)_w$, $(K_w + K_b)_t$, K_2 and k_m are correction factors (for more details about correction factors calculations, refer to Appendix). K_1 is a constant given in Table 2. A_w or (A_t) are defined as the ratio of wing or (tail) area to missile's cross section area. $d\varepsilon/d\alpha$ is the change of downwash angle. The subscripts w and t stands for wing and tail, respectively.

II.2. Drag Force Prediction

The drag on the missile can be divided into several major components, they are: wave drag due to the presence of shock waves and dependent on the Mach number, viscous drag due to friction, induced drag due to the generation of lift, base drag due to the wake behind the missile, interference drag due to the interaction of various flow fields and finally roughness drag due to surface roughness.

For conical fore body the wave drag coefficient from [8] and [10] is:

$$C_{Dwc} = \left(0.083 + \frac{0.096}{M^2} \right) (5.73\theta)^{1.96} \quad (4)$$

Where: θ is the half cone angle in radian as shown in (Fig. 2).

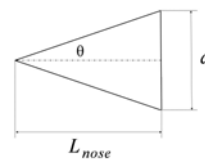


Fig. 2. Conical nose

For parabolic fore body and bodies of close shape the wave drag coefficient from [8] and [10] is:

$$C_{Dwp} = C_{Dwc} \frac{0.08(15.5 + M)}{(3 + M)} \quad (5)$$

This equation is valid for $1.5 \leq M \leq 6$ and $\lambda_{nose} \geq 2.5$, Where $\lambda_{nose} = L_{nose} / d$ is called nose fineness ratio (see Fig. 3).

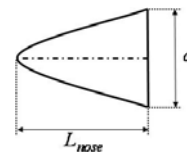


Fig. 3. Parabolic nose

The wave drag coefficient of an isolated, rectangular wing or tails of finite span is [8]:

$$C_{Dw} = \frac{K_1 (t/c)^2}{\sqrt{M^2 - 1}} \left[1 - \frac{1}{2AR\sqrt{M^2 - 1}} \right] \quad (6)$$

Where: t/c is the thickness to chord ratio and K_1 is a constant depending on the type of airfoil and is given in Table 2.

Airfoil Type	K_1
Double Wedge	4
Modified Double Wedge	6
biconvex	5.33

Viscous drag coefficient is the main component at supersonic speeds, from [8] and [11]:

$$C_{Df} = \begin{cases} \frac{1.328}{\sqrt{R}} & R < 10^6 \\ \frac{0.427}{(\log_{10} R - 0.407)^{2.64}} & R > 10^6 \end{cases} \quad (7)$$

Where: R is the Reynolds number based on the wetted area and the length of the missile. For large missiles, turbulent flow can be assumed.

Induced drag coefficient is due to the generation of lift i.e. depending on angle of attack and is approximated by [8]:

$$C_{Di} \cong C_N \alpha \quad (8)$$

Base drag is a function of both the missile flight condition and geometry (i.e. the shape of the missile). The parameters affecting base drag are Reynolds number, Mach number, angle of attack, body's (missile's total length) fineness ratio (L/d), fin proximity, and the presence of boat tail or flare. Reynolds number, angle of attack, body fineness ratio and fin proximity are often ignored because they are negligible. And, in general the contribution of the base drag to the total drag is very small. Thus the base drag coefficient is [10]:

$$C_{Db} = 0.3129e^{-0.38745M} \quad (9)$$

Interference drag is experimentally found to be 5% of the total drag force coefficient [11]:

$$C_{D\text{interference}} = 0.05C_D \quad (10)$$

The total drag force coefficient with interference from [14]:

$$C_D = 1.05 \left[C_{D_{bw}} + 4(C_{Dw})_{wing} A_w + 4(C_{Dw})_{tail} A_t + C_{Df} + C_{Di} \right] \quad (11)$$

The model also account for corrections and interference factors such as: fin body interference, correction for taper ratio, correction for boundary layer effect, correction for not remote wing, influence of flow stagnation, wing tail interference (correction for stagnation), and correction for downwash and interference factors for tail movable area (for the mathematical details, refer to the Appendix).

III. Model Validation and Verification

The analytical aerodynamic model presented in the previous section is completely closed-form technique for calculating the aerodynamic characteristics of a missile. The model gives a good approximation for aerodynamic forces. To ensure the accuracy of the calculations, the results are validated with previous experimental wind tunnel data. Normal force coefficients and axial force coefficients are compared with experimental results.

The wind tunnel experimented data is selected from the study in [12]. The tested model is a cruciform inline canards and aft tails missile shown in Fig. 4. The specifications and test conditions are shown in Table 3,

TABLE 3
TESTED MODEL SPECIFICATIONS AND TEST CONDITIONS

Nose To Diameter Ratio	$L_{nose}/d = 3.$
Cylinder Length To Diameter	$L_{cyl}/d = 12.$
Canards Aspect Ratio	$AR = 1.6$
Canards Taper Ratio	$\lambda = 0.625.$
Tails Aspect Ratio	$AR = 2.33$
Tails Taper Ratio	$\lambda = 0.625.$
Canards And Tails Deflection Angles	$\delta_{canard} = \delta_{tail} = 0$
Testing Mach Number	$M = 1.75.$
Reynolds Number	$Re = 4.33 \times 10^5$ (based on body diameter)
Reference Area	$A_{ref} = 0.25\pi d^2.$
Reference Length	$L_{ref} = d.$
Moment Reference	$x_m/L = 0.49$

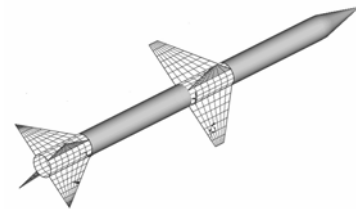


Fig. 4. Testing model used for validation [12]

Fig. 5 and 6 show the comparison results of the analytical aerodynamic model with the wind tunnel experimental data.

It can be observed that the normal force coefficients are in excellent agreement with the experimental data until $\alpha = 10^\circ$. After that the error in the prediction in this method starts to build up gradually and reaches up to 13% at $\alpha = 20^\circ$. The error after $\alpha = 10^\circ$ is expected due to the assumption made of small angle of attack during the formulation of the normal force coefficients equations. Otherwise, without this assumption it is impossible to reach to an analytical prediction.

The axial force coefficients prediction shows good results with the experimental data up to $\alpha = 8^\circ$. The error is justified by two factors: the assumption of small angle of attack in the formulation and the effect of induced drag prediction which is a function of the lift force.

The normal and axial force coefficients accuracy is considered sufficient to be used in missile preliminary design especially for application of small range of angle of attack.

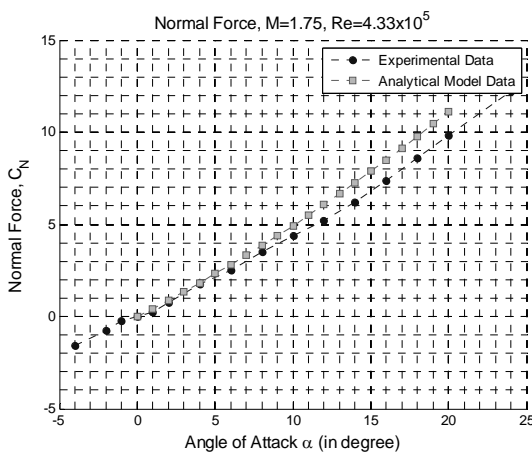


Fig. 5. Normal Force comparison of Experimental, Analytical Model Data

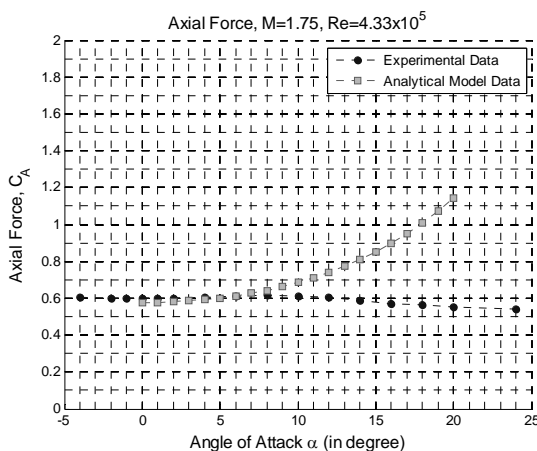


Fig. 6. Axial Force comparison of Experimental, Analytical Model Data

IV. Aerodynamic Shape Configuration Optimization

The aerodynamic configuration sizing parameters that are important in the process of design are: flight condition parameters (angle of attack α , Mach number M , and altitude h), missile's nose fineness ratio L_{nose}/d , missile's diameter, missile's fineness ratio L/d , wing's geometry and size, stabilizer's geometry and size, flight control surface geometry and size (see Fig. 7). In reality, most missiles' flight time is in the supersonic regime and it is comparatively short in subsonic and hypersonic regimes. That is why the objective of this paper is to enhance the aerodynamic shape at supersonic speed only using Monte Carlo optimization method.

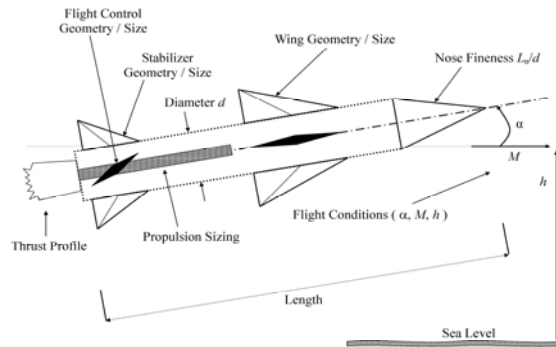


Fig. 7. Aerodynamic configuration sizing parameters summary

IV.1. Monte Carlo Optimization Method

The Monte Carlo method is mainly based on the principle of random numbers. This method can be implemented efficiently using a personal computer, wherein random data is generated for different simulations or processes to draw a statistical conclusion.

To illustrate the concept of random numbers, take the interval $[0, 1]$ and think of a series of real numbers a_1, a_2, \dots lying in the interval. We can conclude that the series is random in nature if the numbers appear to be distributed arbitrarily with no pattern in the progression of the numbers in the interval.

Here we are going to implement this method for optimization by selecting some parameters randomly and checking the cost function to be optimized until optimal solution is reached. The selection of the same randomly generated number is avoided during the optimization process to ensure the optimality of the solution. Finally, the biggest advantage of this method is the avoidance of tumbling in some local minima or

local maxima since most of the regular optimization techniques fall in this cavity resulting in non-optimal or locally optimal.

Monte Carlo simulation has become recognized as an effective and powerful tool for system evaluation in the development of aerospace vehicles. The advantages of the Monte Carlo simulation are [13]: the nonlinear system can be evaluated directly, the results reflect the influences of combinatorial effects of various uncertain parameters and the uncertain parameters can be determined as physical values.

IV.2. Optimization Problem

The optimization is subjected to the geometrical constraints of missile's fineness ratio (L_r), end of nose to wing distance (L_w), exposed wing chord (c_w), exposed wing semi span (b_w), exposed tail chord (c_t) and exposed tail semi span (b_t). The constraints are shown in Fig. 8. The numerical values of these constraints are based on missiles' statistics. It should be noted that all the values are normalized with respect to missile's diameter. Mathematically, the objective function and constraints are expressed as follows:

Maximize (for $1.5 \leq M \leq 6$):

$$f(L_r, L_w, c_w, b_w, c_t, b_t) = \frac{C_L}{C_D} \quad (12)$$

Subjected to the constraints:

$$\begin{aligned} 9.46 &\leq L_r/d \leq 13.34 \\ 2.0 &\leq L_w/d \leq 7.63 \\ 0.20 &\leq c_w/d \leq 0.915 \\ 0.20 &\leq b_w/d \leq 0.61 \\ 0.20 &\leq c_t/d \leq 0.915 \\ 0.20 &\leq b_t/d \leq 0.61 \end{aligned} \quad (13)$$

The optimization code is written and run using Matlab. The code implements the Monte Carlo optimization technique and varies the Mach number from $M = 1.5$ to 6, and the angle of attack from $\alpha = 0^\circ$ to 8° . The block diagram for the optimization process is clearly shown in Fig. 9.

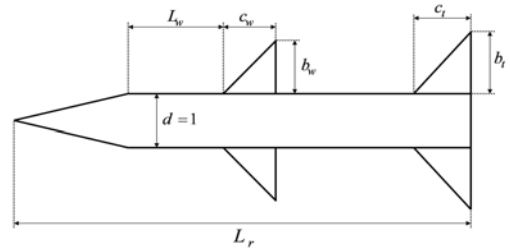


Fig. 8. Optimization parameters

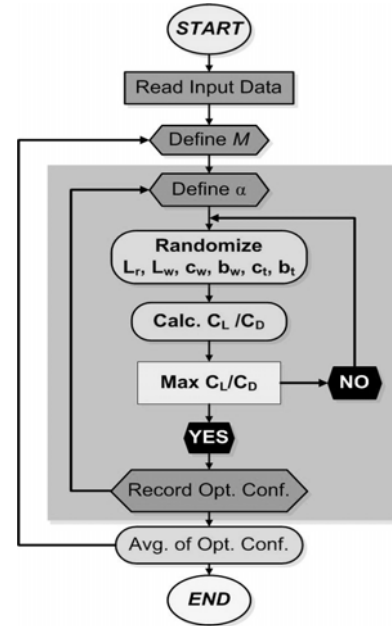


Fig. 9. Optimization process block diagram

V. Optimization Results

The results are shown in Fig. 10 to 14. The optimal results are summarized in Table 4. For all cases of Mach number, it is found that the wing configuration is the same and the tail configuration is the same again. The size of tail is larger than the wing by almost 11 times. Having small wing is contributing heavily in enhancing C_L/C_D by reducing the drag incredibly by the following factors:

- Reduction of the wing wave drag since the wave drag is inversely proportional to the wing aspect ratio.
- Reduction of the viscous drag.
- Reduction of the induced drag since the lift generated is reduced.
- Smaller wing on tail interference, interference is a function of wing semi span.
- Reduction of the downwash effect, which enhances the tail's performance in terms of generating efficient lift.

The wing's location does not play significant role for enhancing C_L/C_D for all supersonic speeds. The

missile's fineness ratio change does not show correlation with the change of Mach number. Finally, the optimal shapes obtained at each Mach number are closely similar, so an average shape (i.e. averaging each parameter) is selected (Table 4).

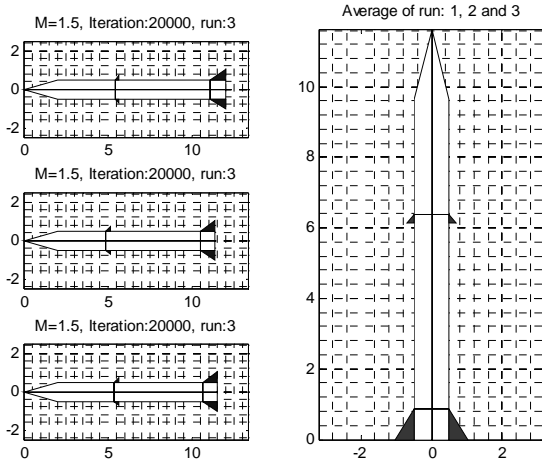


Fig. 10. Optimal Missile Configuration at $M = 1.5$

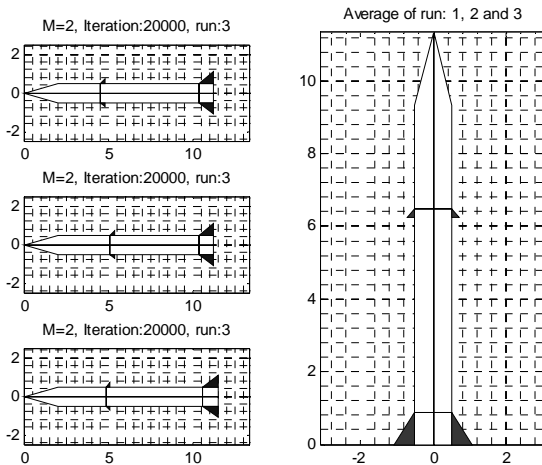


Fig. 11. Optimal Missile Configuration at $M = 2$

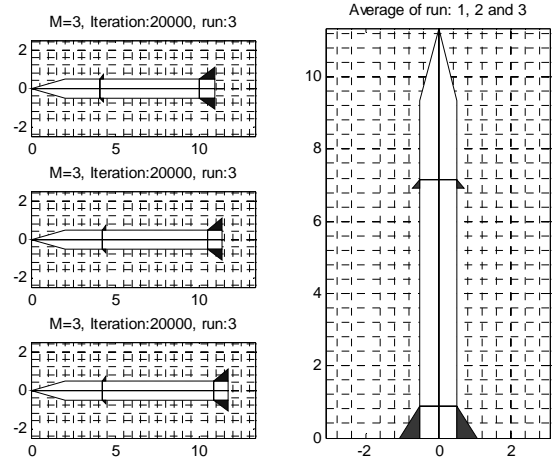


Fig. 12. Optimal Missile Configuration at $M = 3$

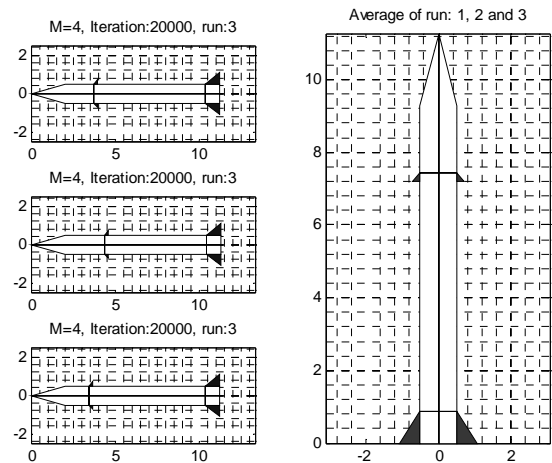


Fig. 13. Optimal Missile Configuration at $M = 4$

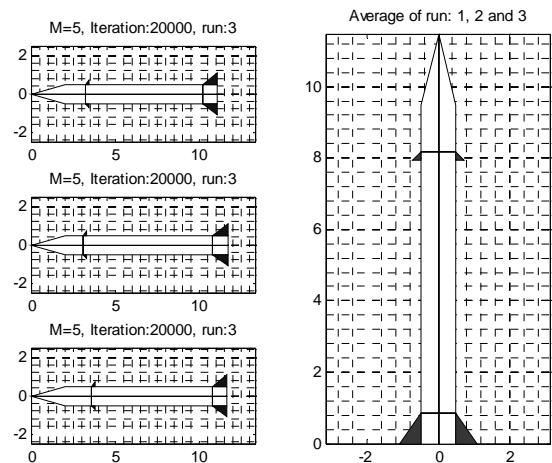


Fig. 14. Optimal Missile Configuration at $M = 5$

TABLE 4

MISSILE CONFIGURATION OPTIMAL RESULTS						
<i>M</i>	1.5	2	3	4	5	Average
b_w	0.204	0.201	0.205	0.205	0.209	0.205
b_t	0.593	0.591	0.581	0.585	0.577	0.587
c_w	0.218	0.219	0.222	0.229	0.228	0.224
c_t	0.877	0.889	0.893	0.887	0.889	0.883
L_c	9.435	9.925	9.499	9.026	9.497	9.485
L_w	4.859	5.087	4.351	2.789	2.659	3.657
L_r	11.435	11.925	11.499	11.026	11.497	11.485
$(C_l/C_D)_{max}$	2.888	2.693	2.634	2.627	2.387	

VI. Conclusion

For supersonic speeds and operating angle of attack in the range $\alpha = 0^\circ$ to 8° , build up components method can be used effectively as a fast method for predicting aerodynamic forces coefficients. The prediction of the normal force coefficients is more accurate than the drag coefficients. The drag prediction is acceptable for small angle of attack. The missile shape configuration can be optimized using Monte Carlo technique and lift over drag as the cost function. The proposed technique is very fast, efficient, and the resulting missile shapes are comparable with actual operating missiles. Future research would include multi objective cost function and other optimization techniques.

Appendix

Fin Body Interference: fins (wings or tails) body interference can be defined by the following parameters:

- $C_{Nb}(t)$, $C_{Nb}(w)$: normal force coefficient increment for the body in the presence of the tail and wing, respectively.
- $C_{Nt}(b)$, $C_{Nw}(b)$: normal force coefficient for the tail and wing in the presence of the body, respectively.

If C_{Nt} is the normal force coefficient of tail in the absence of the body and C_{Nw} is the normal force coefficient of wing in the absence of body then, interference factors are defined as [11]:

$$k_w = \frac{C_{Nt}(b)}{C_{Nt}} = \frac{C_{Nw}(b)}{C_{Nw}}$$

$$k_b = \frac{C_{Nb}(t)}{C_{Nt}} = \frac{C_{Nb}(w)}{C_{Nw}}$$

Where: k_w is the Normal force coefficient interference for fin due to the presence of body and k_b is Normal force coefficient interference for body due to the presence of fin.

It has been found that these interference factors are function of the ratio r/S_m , where, r is the body radius and S_m is the semi span of fin including the body, see Fig. 15.

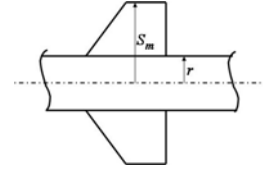


Fig. 15. Fin-body interaction

Defining the ratio $S = S_m / r$, So that the fin-body interferences i.e. wing-body or tail-body are:

$$k_b = \frac{2}{\pi(S-1)^2} \times \left[\frac{\pi(S^2-1)^2}{4S^2} - \frac{(S^2-1)}{S} + \frac{(S^2-1)^2}{2S^2} \sin^{-1} \left(\frac{S^2-1}{S^2+1} \right) \right] \quad (14)$$

$$k_w = \frac{2}{\pi(S-1)^2} \times \left[\frac{\pi(S^2-1)^2}{4S^2} + \frac{(S^2-1)}{S} + \frac{(S^2-1)^2}{2S^2} \sin^{-1} \left(\frac{S^2-1}{S^2+1} \right) \right] \quad (15)$$

Correction for Taper Ratio: Experimental investigations have established that theoretical formulas for k_w , k_b helps to obtain good results for the interference of a wing with rectangular panels for which the taper ratio $\lambda = c_r/c_t$ (c_r , c_t are the root and tip chord respectively Fig. 16). Increasing taper ratio ($\lambda > 1$) leads to larger interference factors. Experiments showed that these factors are virtually the same for k_w , k_b and can be assumed to be equal [11]:

$$v_{b,\eta} = v_{w,\eta} = v_\eta = 1 + \frac{r_m(1-r_m)}{(1+r_m)^2} \left(1 - \frac{1}{\lambda} \right) \quad (16)$$

Where: $r_m = r/S_m$.

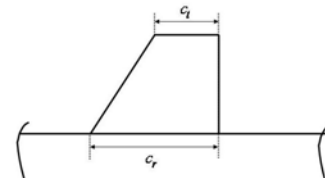


Fig. 16. Fin configuration

Correction for Boundary Layer Effect: this influence manifests itself in the change in the effective radius of the body where the panels are moved by the value of the displacement thickness of the boundary layer δ^* . Using this value of the new radius $r^* = r + \delta^*$ and the

parameter $r_m = r^*/S_m$ (Fig. 17) we determine the new interference factor. Its value allows us to calculate the correction factors for k_w , k_b which is assumed to be identical [11],

$$v_{b.bt} = v_{w.bv} = v_{bt} = \frac{r_m (1+r_m^2) [r_m + r_m (1+3r_m) - 1] \bar{\delta}^*}{1 - \frac{r_m (1+r_m^2) [r_m + r_m (1+3r_m) - 1] \bar{\delta}^*}{\lambda}} \quad (17)$$

Where: $\bar{\delta}^* = \delta^*/r$, $\delta^* = 0.125(0.37/R_{L_1}^{0.2})L_1$, $L_1 = X_w + 0.5c_r$ and R is the Reynolds number based on the length L_1 (see Fig 17).

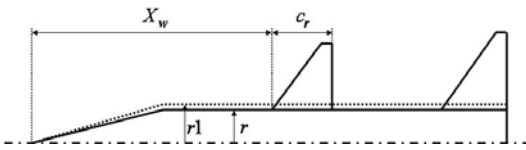


Fig. 17 Missile's Boundary Layer

Correction for Not Remote Wing: k_w , k_b were obtained by assuming that the wing is located sufficiently remote from the nose, and therefore, the latter (together with the cylindrical part) does not virtually affect the flow over the wing. When the wing is not far from the nose, the influence of the part of the body ahead of it may be appreciable. Investigations [11] show that the interference factor here decreases by a certain factor seen below,

$$v_{b.f} = v_{w.f} = v_f = e^{0.05(1-M_\infty)} \quad (18)$$

And is valid for Mach number $M_\infty \leq 5$.

Influence of Flow Stagnation: the aerodynamic calculation of the body wing combination considered above was performed while assuming that the wing is in a flow that does not practically differ from an undisturbed one. An actual flow is characterized by stagnation of the flow ahead of the wing that must be taken into consideration while determining the aerodynamic parameters. The degree of this stagnation can be characterized by the mean stagnation coefficient $K_1 = q/q_\infty$ for which is $q = \gamma P M_1 / 2$ found from an average value of the Mach number M_1 of the disturbed flow ahead of the wing. Assuming the pressure in the disturbed and undisturbed flows to be the same ($P = P_\infty$) then, $K_1 = M_1^2 / M_\infty^2$. If the wing is at a distance $X_w > 1.5L_{nose}$ from the tip of a nose having the form of a cone with semi apex angle $\beta_c < \beta_{cr}$ (where β_{cr} is the critical value of this angle) then K_1

can be calculated as:

$$K_1 = \frac{M_1^2}{M_\infty^2} = \frac{2}{M_\infty^2 (\gamma - 1)} \left[v_o \frac{(\gamma - 1)}{\gamma} \left(1 + \frac{\gamma - 1}{2} M_\infty^2 \right) - 1 \right] \quad (19)$$

Where

$$v_o = \left(\frac{\gamma + 1}{2} \right)^{\frac{\gamma + 1}{\gamma - 1}} \left[\frac{X^2}{1 + (\gamma - 1)/2X^2} \right] \left[\gamma X^2 - \frac{\gamma - 1}{2} \right]^{-\frac{\gamma}{\gamma - 1}},$$

$$X = 1 - \cos \beta_c + \left(1 + \frac{\gamma - 1}{2} M_\infty^2 \sin^2 \beta_c \right)^{\frac{1}{2}}$$

It should be noted that if the nose part differs from a conical one K_1 can be calculated as follows:

- 1) Find C_{X_w} for the given nose from the relevant aerodynamic relations.
- 2) Use the following equation to evaluate the corresponding semi-apex angle β_c of a conditional conical surface which will replace the given nose:

$$\beta_c = \left(\frac{C_{X_w}}{2 \times 10^{-9} (0.8 + M_\infty^{-2})} \right)^{0.588}$$

- 3) Calculate K_1 .

Wing Tail Interference (correction for Stagnation): the effectiveness of a tail unit depends on the flow stagnation due to the nose and wings ahead of the tail [10] and [11]. The correction factor is given by:

$$K_2 = K_1 \left(\frac{K^1 + \bar{S}_t}{1 + S_t} \right) \quad (20)$$

Where: $\bar{S}_t = S_t / S_w$, S_t is the tail area and S_w is the wing area. The values of K^1 are given in Fig. 18 where X_{cm} is distance from the wing's trailing edge to tail's center of mass.

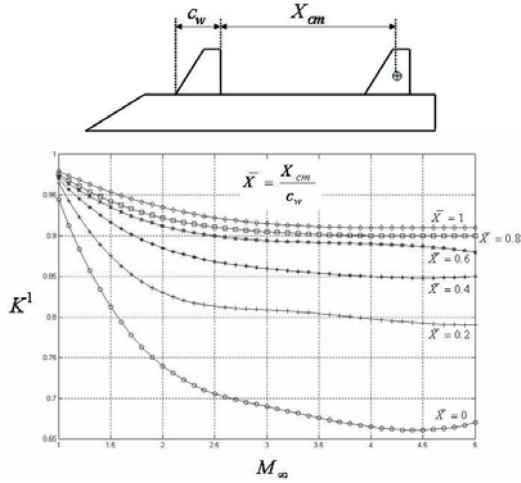


Fig. 18. Values of K^1

Correction for Downwash: it is known that the downwash effectively reduce the angle of incidence at the tail, hence we should account for this effect [10] and [11]. The change of the downwash angle,

$$\left(\frac{d\varepsilon}{d\alpha}\right)_t = (1 - \eta_t) \Delta\varepsilon \quad (21)$$

Where: $\Delta\varepsilon = S'_t/S_t$, S'_t is the tail area inside the mach cone and

$$\eta_t = 1 + \frac{i_c K_w C_{Ntd} S_w}{8\pi (K_w + K_b)_t [(S_m)_t - r] (Z_v - r)}$$

Also,

$$i_c = \frac{-4Z_v [(\bar{S}_m)_t - r] (K_w)_t}{(\bar{Y}_v^2 + \bar{Z}_v^2) (\bar{S}_m)_t},$$

$$\bar{Z}_v = \frac{Z_v}{(S_m)_t}, \bar{Y}_v = \frac{Y_v}{(S_m)_t},$$

$$Z_v \approx r + (S_m - r) [0.885 + 0.2049(r_m + 0.5) + 0.1072(r_m + 0.5)^2],$$

$$(\bar{S}_m)_t = \frac{(S_m)_t}{r} \text{ and } Y_v = 2.75(X_{cm})_t$$

Interference Factors for Tail Movable Area: two interference factors will be accounted for if having movable tails [10] and [11],

$$k_{w_m} = \frac{k_w^2}{1 + r_m} \quad (22)$$

$$k_{b_m} = k_w - K_W \quad (23)$$

Finally, the related interferences and correction

factors are multiplied together for the corresponding component,

$$(K_w + K_b)_w = \left(k_w \cdot v_{b,\eta} \cdot v_{w,bv} \cdot v_{w,f} + \right) \left(k_b \cdot v_{w,\eta} \cdot v_{b,bt} \cdot v_{b,f} \right)_w \quad (24)$$

$$(K_w + K_b)_t = \left(k_w \cdot v_{b,\eta} \cdot v_{w,bv} \cdot v_{w,f} + \right) \left(k_b \cdot v_{w,\eta} \cdot v_{b,bt} \cdot v_{b,f} \right)_t \quad (25)$$

Acknowledgements

The authors would like to acknowledge the support of King Fahd University of Petroleum and Minerals, Dhahran, Saudi Arabia.

References

- [1] Micheal J. Hensch, Jack N. Nielsen, *Tactical Missile Aerodynamics*, Progress in Astronautics and Aeronautics; V.124, (American Institute of Aeronautics and Astronautics, Inc, 1992).
- [2] S. S. Chin, *Missile Configuration Design*, (McGraw Hill Book Company, 1961).
- [3] Eugene L. Fleeman, *Tactical Missile Design*, 2nd edition, (AIAA Education Series, 2006).
- [4] J. Roshanian, Z. Keshavarz Effect of Variable Selection on Multidisciplinary Design Optimization a Flight Vehicle Example, *Chinese Journal of Aeronautics*, pp.86-96, 2006.
- [5] Thomas J. Sooy, Rebecca Z. Schmidt, Aerodynamic Predictions, Comparison and Validatind Using Missile DATCOM (97) and Aeroprediction 98 (AP98). *Journal of Spacecraft and Missiles*, Vol. 42, No. 2, pp.257-265, March, 2005.
- [6] Ward Cheney and David Kincaid, *Numerical Mathematics and Computing*, (Brooks/Cole Publishing Company, 1999).
- [7] G. Kjellström, Useful Monte Carlo optimization, *Journal of Optimization Theory and Applications*, Volume 69, Number 1 / April, 1991.
- [8] J. W. Cornelisse, H. F. R. Schoyer, K. F. Wakker, *Rocket Propulsion and Spaceflight Dynamics*, (Pitman Publishing Limited, 1979).
- [9] George M. Siouris, *Missile Guidance and Control Systems*, (New York, Springer, 2004).
- [10] USAF DATCOM, 1970.
- [11] N. F. Kvasnov, *Aerodynamics I, II*, (1980).
- [12] D.. Lesieutre, John F. Love, Marnix F. E. Dillenius, Prediction of the Nonlinear Aerodynamic Characteristics of Tandem-Control and Rolling-Tail Missiles, *AIAA 2002-4511*, August, 2002.
- [13] Toshikazu Motoda, Simplified Approach to Identifying Influential Uncertainties in Monte Carlo Analysis. *Journal of Spacecraft and Missiles*, Vol. 41, No. 1, pp.1071-1074, November, 2004.
- [14] Ayman M. Abdallah, *On Rocket Performance, Stability and Control*, Master thesis, Aerospace Eng. Dept., King Fahd University Of Petroleum & Minerals, Dhahran, 2007.

Authors' information

¹King Fahd University of Petroleum and Minerals, Dhahran 31261, Saudi Arabia.

²King Fahd University of Petroleum and Minerals, Dhahran 31261, Saudi Arabia.

³King Fahd University of Petroleum and Minerals, Dhahran 31261, Saudi Arabia.



Ahmed Z. Al-Garni holds PhD in Aerospace Engineering (Flight Dynamics and Control in the Atmosphere and Space) from the University of Maryland, College Park, Maryland, USA, 1991. Area of specialization includes Flight Dynamics and Control in Air and Space, Aerodynamics, Astrodynamics and Aerospace Design. Currently, he is Professor and Chairman of Aerospace Engineering Department in King Fahd University of Petroleum and Minerals Dhahran, Saudi Arabia. Dr. Al-Garni is a Senior Member in AIAA.



Ayman H. Kassem holds PhD in Aerospace Engineering from Old Dominion University, Virginia, USA, 1998. Area of specialization includes Flight Dynamics and Control, Guidance and Navigation, Space Dynamics, Optimization and Flight Structures. Currently, he is Assistant Professor in Aerospace Engineering Department in King Fahd University of Petroleum and Minerals Dhahran, Saudi Arabia. Dr. Kassem is a Member in AIAA.



Ayman M. Abdallah holds M.S. in Aerospace Engineering from King Fahd University of Petroleum and Minerals, Dhahran, Saudi Arabia, 2007. Area of specialization includes Flight Dynamics and Control, Astrodynamics and Aerospace Optimization. Currently, he is Graduate Assistant in Aerospace Engineering Department in King Fahd University of Petroleum and Minerals Dhahran, Saudi Arabia. Mr. Abdallah is a Member in AIAA.